Chemistry and Physics of Lipids 225 (2019) 104792

Contents lists available at ScienceDirect

Chemistry and Physics of Lipids

journal homepage: www.elsevier.com/locate/chemphyslip

Combining nuclear magnetic resonance with molecular dynamics simulations to address sumatriptan interaction with model membranes

Irene Wood[a,b,*,1], Lucas Fabian[c], Albertina Moglioni[c,d], Luis Fernando Cabeça[e], Eneida de Paula[f], Mónica Pickholz[a,b]

[a] Departamento de Física, Facultad de Ciencias Exactas y Naturales, Universidad de Buenos Aires, Buenos Aires, Argentina
[b] Instituto de Física de Buenos Aires (IFIBA) (UBA-CONICET), Argentina
[c] Instituto de la Química y Metabolismo del Fármaco (IQUIMEFA) (UBA-CONICET), Argentina
[d] Departamento de Farmacología, Facultad de Farmacia y Bioquímica, Universidad de Buenos Aires, Buenos Aires, Argentina
[e] Departamento de Química, Univ. Federal Tecnológica do Paraná, Londrina, PR, Brazil
[f] Departamento de Bioquímica e Biologia Tecidual, Instituto de Biologia, Universidade Estadual de Campinas (Unicamp), CP 6109, CEP 13083-970, Campinas, SP, Brazil

ARTICLE INFO

Keywords:
Sumatriptan
Nuclear magnetic resonance
Membranes
Molecular dynamics
Liposomes

ABSTRACT

The goal of this work is to obtain a complete map on the interactions between sumatriptan, an amphiphilic ionizable anti-migraine drug, with lipid bilayers. To this end, we combined two physico-chemical techniques – nuclear magnetic resonance and molecular dynamics simulations – to obtain a detailed picture at different pH values. Both approaches were used considering the strength and constraints of each one. NMR experiments were performed at pH 7.4 where at least 95% of the drug molecules are in their protonated state. From NMR, sumatriptan shows partition on the interfacial region of model membranes (near the head groups and intercalating between adjacent lipids), inducing changes in chemical environment and affecting lipid dynamics of liposomes, in a dose dependent manner. Due to the experimental instability of lipid bilayers at high pH, we took advantage of the molecular dynamics power to emulate different pH values, to simulate sumatriptan in bilayers including at fully uncharged state. Simulations show that the neutral species have preferential orientation within the bilayer interface while the distribution of protonated drugs is independent on the initial conditions. In summary, several properties depicted the interfacial partition of the anti-migraine drug at the water-lipid interface at different conditions. Both techniques were found complementary to shed light on the structural and dynamics of sumatriptan-lipid bilayer interactions.

1. Introduction

Triptans are synthetic drugs used for migraine treatment (Negro et al., 2018). They act as selective agonists on some subtypes of 5-HT1 receptors, most of which are located at the central nervous system (Filip and Bader, 2009). In order to reach these central receptors and exert their pharmacological effect, triptans must cross biological interfaces, as the blood-brain barrier (BBB) (Ahn and Basbaum, 2005; Edvinsson and Tfelt-Hansen, 2008). Sumatriptan (SMT) is the pharmacological prototype and first designed triptan (Johnston and Rapoport, 2010). Other triptans were designed after SMT (Tfelt-Hansen et al., 2000), looking to improve pharmacokinetic profile and permeation and to reduce adverse effects. Even that, SMT is nowadays still considered one of the most efficient drugs among its family. In this sense, it is important to obtain physical-chemical understanding, at high-resolution and molecular level, of SMT interaction with model membranes, in order to get insights on its effects on simplified models of biological barriers.

Usually, neutral compounds have greater membrane partition (given their higher *n*-octanol/water partition) than charged ones

Abbreviations: Alip, area per lipid; BBB, blood-brain barrier; ΔCS, chemical shift change; EDP, electron density profile; EPC, egg phosphatidylcholine; g(r), radial distribution function; Ka, ionization constant; Kp, partition constant; POPC, palmitoyl-oleoyl-phosphocholine; logP, partition coefficient; POPC, palmitoyl-oleoyl-phosphocholine; MD, molecular dynamics; NMR, nuclear magnetic resonance; NOE, nuclear Overhauser effect; POPC, palmitoyl-oleoyl-phosphocholine; ROESY, rotating-frame nuclear Overhauser effect correlation spectroscopy; SMT, sumatriptan; T_1, longitudinal relaxation times

* Corresponding author at: Departamento de Física, Facultad de Ciencias Exactas y Naturales, Universidad de Buenos Aires, Buenos Aires, Argentina.
E-mail address: irenewood@fmed.edu.uy (I. Wood).
[1] Current address: Departamento de Bioquímica – Centro de Investigaciones Biomédicas (CEINBIO), Facultad de Medicina, Universidad de la República (UDELAR), Gral. Flores 2125, CP11800, Montevideo, Uruguay.

https://doi.org/10.1016/j.chemphyslip.2019.104792
Received 26 March 2019; Received in revised form 21 June 2019; Accepted 17 July 2019
Available online 27 July 2019
0009-3084/

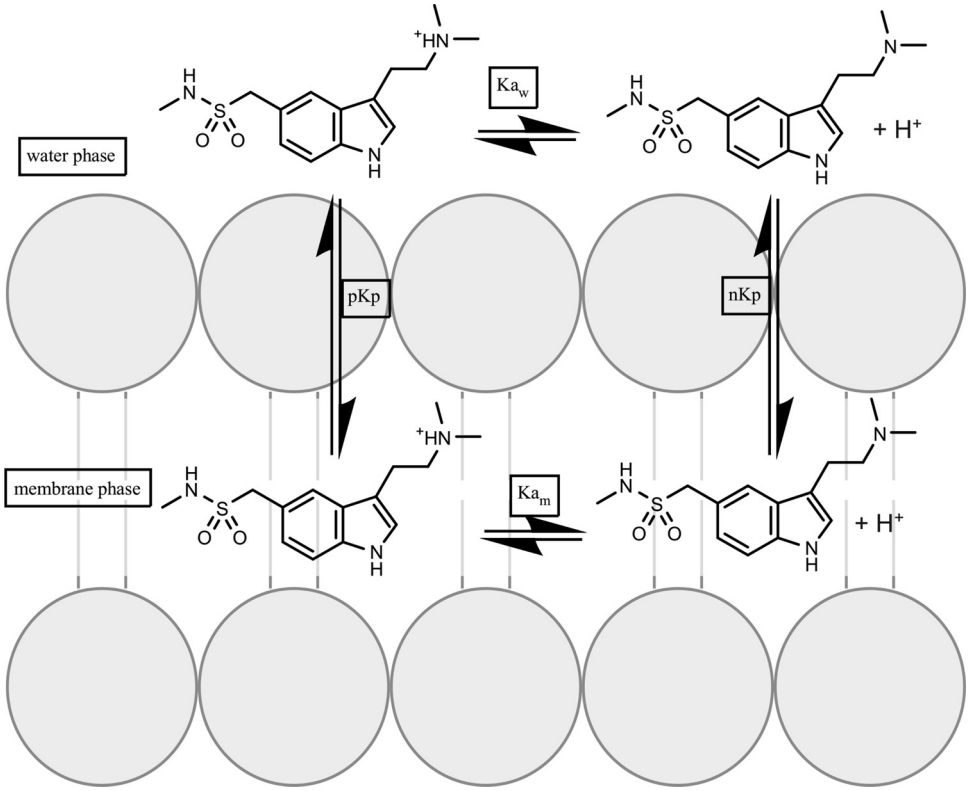

Fig. 1. Scheme of SMT ionization and partition between water and membrane phases. K_a and K_p are the ionization and partition equilibrium constants, respectively. "p" and "n" refer to the protonated and neutral species of sumatriptan; "w" and "m" refer to water and membrane phases.

(Avdeef et al., 1998). Besides, the partition coefficient determined between *n*-octanol/water phases could be different from that between membranes/water (de Paula and Schreier, 1996; Gregoriadis, 1992). This fact is due to the bidimensional molecular organization of lipids in bilayers and also because the ionization constant (K_a in Fig. 1) of amphiphiles in the presence of non-homogeneous media such as membranes can change, reflecting the different partition constant (K_p) of the charged/uncharged species.

Since the pKa of SMT is ˜9.7 (Wellcome, 2001; Wojnar-Horton et al., 1996), the prevalent ionization specie at physiological pH is the protonated one (Wellcome, 2001; Wojnar-Horton et al., 1996; Wood and Pickholz, 2013). Although at physiological pH most of SMT molecules are in the protonated form, it is important to understand the behavior of both charged and uncharged species in the membrane. Nevertheless, to reach neutral SMT (pH ≈ 12) state in bilayers is not feasible by experiments, due to the structural changes of the lipid structure at this pH, caused by deprotonation of the choline amine group (Austin et al., 2005, 1995; Boggara and Krishnamoorti, 2010; Boggara et al., 2012). In this context, computer simulations appear as a very powerful tool to fill this gap.

Previously, we have reported through Molecular Dynamics (MD) at different scales –atomistic and coarse grain-, that SMT in its protonated form (pSMT), showed interfacial distribution in palmitoyl-oleoyl-phosphocholine (POPC) bilayers (Wood et al., 2018; Wood and Pickholz, 2013, 2014). pSMT molecules were seen to partition between the aqueous and lipid/water interface, with no access to the hydrophobic membrane core. These results are in good agreement with low *n*-octanol/water partition coefficient (logP < 1) (Shidhaye et al., 2008; Tfelt-Hansen, 2010) and biopharmaceutical classification systems (Dave and Morris, 2016; Tanaka et al., 2017), suggesting SMT high affinity for polar phases (Shidhaye et al., 2008). Notwithstanding, in our simulations SMT showed high interaction with the lipid headgroups, indicating that such traditional classifications may offer a biased and poorly detailed estimation of drug affinity for different phases, as previously suggested in the literature (Avdeef et al., 1998; Bemporad et al., 2005; Santos et al., 2003). The limitations of pSMT molecules to diffuse through membranes have been related to specific groups involved in interactions with either the polar head-groups and water, as well as to the high electric and atomic density of the interfacial region (Wood and Pickholz, 2013).

Nuclear Magnetic Resonance (NMR) is a powerful tool to study molecular structure and dynamics, giving valuable experimental information on the interaction of small solutes with model membranes (Cabeça et al., 2009; Fraceto et al., 2005; Gawrisch et al., 2002). From NMR spectra, differential changes in the chemical shifts, longitudinal relaxation times and intermolecular through the space -nuclear Overhauser effect (NOE)- interactions can be obtained, unraveling the topology of drug-bilayer interaction (Gawrisch et al., 2002; Kuroda and Fujiwara, 1987; Kuroda and Kitamura, 1984).

Numerous reports in the literature describe the behavior of drugs in model membranes using different approximations (Bemporad et al., 2005; Cabeça et al., 2009; Coimbra et al., 2018, 2014; Fraceto et al., 2005; Hoff et al., 2005; Jemioła-Rzemińska et al., 2005; Kopeć et al., 2013; Paquet et al., 2002; Peetla et al., 2010; Venable et al., 2019). In this context, both MD simulations and biophysical experiments could give a detailed picture of SMT dynamical performance across membrane interfaces (Lopes et al., 2017) and other amphiphilic systems, such as micelles (Wood et al., 2018).

In the present work, we used theoretical (MD) and experimental (NMR) approaches to study SMT interaction (conformation and dynamics) with model phospholipid membranes and to achieve a broad set of stable conditions. Additionally, the advantages and limitations of each approach is discussed, since both NMR and MD results may be compared in some cases, in order to validate results. Then, in the present work, the goal is to show them as complementary tools, finally depicting that the strengths of both techniques may reciprocally complemented to give a complete map of the interactions occurring between drug and lipids in the bilayer system (Cabeça et al., 2009;

Coimbra et al., 2014; Wormald et al., 2002).

2. Materials and methods

2.1. Reagents

Egg phosphatidylcholine (EPC) was obtained from Avanti Polar Lipids (Alabaster, AL, USA) and deuterated water (D_2O, 99.9%) was obtained from Sigma Chemical (St. Louis, MO, USA). Sumatriptan succinate was gently donated by LAFEDAR (Paraná, ER, Argentina). All other reagents were of analytical grade.

2.2. Model membranes

We chose PC bilayers since are used as model membranes for the study of solute membrane permeability and because phosphatidylcholine is the predominant lipid class in mammal endothelial membranes (Carpenter et al., 2014; Chew et al., 2008; Selivonchick and Roots, 1977), such those of BBB. However, it is important to notice the simplicity of our model, considering the complex molecular composition of BBB membranes, e.g. the presence of different classes of lipids, including other phospholipids, sphingolipids and cholesterol and the presence of efflux and other proteins (Campbell et al., 2014).

2.3. Liposomes preparation

Liposomes were obtained as previously described (Fraceto et al., 2002; Fraceto et al., 2005). Shortly, small unilamellar vesicles were obtained by sonication of multilamellar vesicles, suspended in D_2O (pH 7.4). Knowing the partition coefficient of SMT, the drug was added to the sonicated EPC vesicles up to 1:1 molar ratio.

2.4. Nuclear magnetic resonance measurements

^{1}H NMR spectra were obtained with Bruker 600 UltraShield (14.1 T, ^{1}H 600 MHz) equipment. The samples were degassed to avoid the interference of dissolved O_2 during inversion-recovery measurements. The 90° pulse was typically 10–15 μs, and the recycling time was set to 6 s which corresponds to 5 times the largest longitudinal relaxation times (those of the aromatic indole hydrogen nuclei) (Fraceto et al., 2005). Longitudinal relaxation times were obtained by the conventional inversion-recovery technique, at room temperature (Smith and Oldfield, 1984; Wohlert and Edholm, 2006). NOE experiments were conducted using the rotating-frame nuclear Overhauser effect correlation spectroscopy (ROESY) sequence, with 50 ms mixing times, for the detection of NOEs (Gerothanassis et al., 2002; Gil and Geraldes, 1987). Different systems were studied: pure SMT, pure EPC, and SMT:EPC mixtures at 1:3; 1:2 and 1:1 drug:lipid molar ratios, at pH 7.4.

2.5. Molecular dynamics simulations

The simulated model membrane was a POPC bilayer. Each bilayer contained 150 POPC molecules (75 in each leaflet) fully hydrated with 5000 water molecules. Four simulations were carried out, as single replica, considering a 1:3 drug:lipid molar ratio. In Table 1 we summarized the systems, where different pH were emulated: low pH (only pSMT), high pH (only nSMT), and pH of 9.7 (half nSMT and half pSMT). In three of the simulations the drugs were initially placed in the water phase, and in most of the work we will discuss these cases. Besides, we have added an extra case, where protonated drugs were original placed in the lipid core. We will make explicit reference when we refer this case.

The initial coordinates were built up using the Packmol package (Martinez et al., 2009). The simulations were performed using the NAMD2 program (Kalé et al., 1999) within the CHARMM27 force field (Feller and MacKerell, 2000; MacKerell et al., 1998). In relation to the used force field (FF), we are aware that CHARMM36 FF is the current one. Nevertheless, we have used CHARMM27 in order to be consistent with our previous simulations (Wood and Pickholz, 2013, 2014, 2016). The TIP3P model (Jorgensen et al., 1983) was used for water molecules. Both pSMT and nSMT were considered as fully flexible molecules. As for pSMT, nSMT parameters were based on the CHARMM force field, adjusting charge distributions as performed for similar molecules (Wood and Pickholz, 2013, 2014). Topology of nSMT and pSMT is provided in supplementary material.

Table 1
Summary of the four simulated systems considered in this study: we described the number of protonated and neutral drugs in the system, their initial condition (IC) and the simulation run time.

System name	Nº pSMT	Nº nSMT	Run time	IC
pSMT	50	0	150 ns	Water
npSMT	25	25	150 ns	Water
nSMT	0	50	150 ns	Water
pSMTc	50	0	150 ns	Lipid core

The simulations were performed within the NPT ensemble, considering periodic boundary conditions. The temperature was kept constant at 310 K, by means of a Langevin thermostat, applying friction and random force (Andersen, 1980). The Langevin thermostat was used without coupling to hydrogen atoms and with a damping coefficient of 1/ps. In addition, pressure was maintained at 1 atm by using a Langevin barostat (Feller et al., 1995) with a piston period of 5 ps and a damping time of 5 ps. A multiple-time step algorithm, RESPA (Tuckerman et al., 1991), was used, with a shortest time step of 2 fs. The short range forces were computed using a cut-off of 10 Å, and the long-range forces were taken into account by means of the particle mesh *Ewald* technique (Essmann et al., 1995).

3. Results

3.1. NMR evidence of sumatriptan interaction with EPC liposomes at physiological pH

Taking into account the pKa of SMT, results of experiments performed at pH 7.4 are mostly attributable to the charged SMT specie (at least 95% of the total drug population even considering pKa changes within bilayer) (see Fig. 1) (Schreier et al., 1984; de Paula and Schreier, 1996; Zhang et al., 2007). As a first approach the hydrogen NMR spectrum (^{1}H NMR) of SMT and EPC liposomes were collected and their hydrogen nuclei assigned and compared with a predictor tool of NMR software (MestreNova, MestreLab Research) and published spectra. The spectrum of 1:1 SMT:EPC sample was collected and changes in chemical shift (ΔC.S., ppm) of the different peaks were determined, in comparison to SMT and EPC reference samples, as shown in Figs. 2 and 3. For assignment purposes, the structures of SMT and POPC, one of the prevalent lipids in EPC, are given as reference in Fig. 2. Lowercase and uppercase letters indicate the peaks corresponding to SMT and EPC hydrogen nuclei, respectively. The peak at 4.7 ppm correspond to the signal of remaining water hydrogen nuclei in D_2O, the peak assigned as **a** (2.3 ppm) in the SMT spectrum corresponds to succinate hydrogen nuclei and the sharp peak assigned as * corresponds to acetone trace in tube (Fulmer et al., 2010). The assignment of EPC hydrogen nuclei is in good agreement with available spectra, as well as that of SMT (Fraceto et al., 2002; Fraceto et al., 2005; Udutha et al., 2018), confirming the purity of the compounds. The C.S. and ΔC.S. for all peaks in pure samples and mixtures (at 1:3, 1:2 and 1:1 drug:lipid molar ratios) are given in Table S1 (Supplementary material). Also, the spectra corresponding to lower SMT:EPC ratios (1:3 and 1:2) can be seen in Fig. S1.

SMT:EPC spectrum revealed changes in the chemical shifts (in comparison to pure SMT and EPC spectra), for peaks belonging to the drug and lipid. Displacements (ΔC.S.) higher than 0.05 ppm are

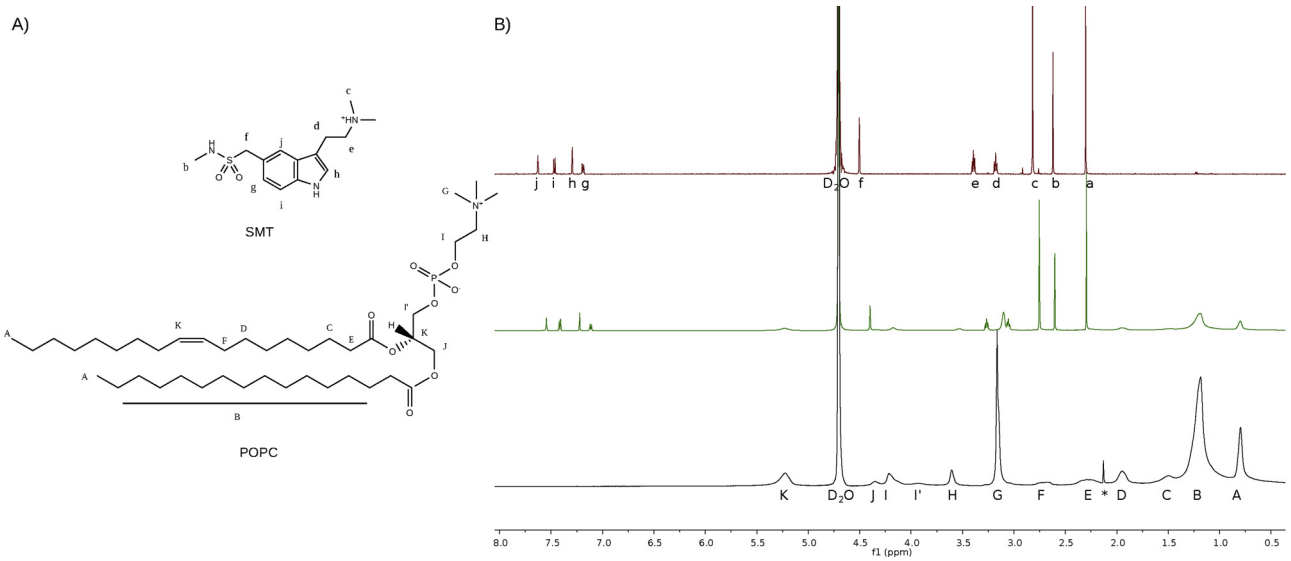

Fig. 2. A) Structures and assignments of SMT and POPC (representative of a typical EPC lipid). B) ^{1}H NMR spectrum of SMT (red, up), SMT:EPC 1:1 (green, middle) and EPC (black, bottom). The sharp peak assigned as * corresponds to acetone trace in tube.

considered significant and representative of changes in the chemical microenvironment of hydrogen nuclei (Cabeça et al., 2009; Fraceto et al., 2002; Fraceto et al., 2005).

Fig. 3 shows significant displacements for SMT peaks: **e–j** (see note in Fig. 3) and for the **H** peak of EPC, indicating changes in the chemical environment of drug and polar head group lipid hydrogen nuclei. It is important to notice that only the peaks not affected by overlapping were plotted in Fig. 3, although Table 1S shows evidences of other SMT (**c** and **d**) and EPC (**G**) peaks shifted towards lower chemical shift values, suggesting a greater shielding of nuclei caused by the change of environment upon drug insertion into the membrane (Fraceto et al., 2002; Fraceto et al., 2005). Fig. 3 also shows the effect of increasing SMT concentrations on the chemical shift of both SMT and EPC signals. At the experimental condition, SMT molecules are distributed in the water and in the membrane phases, so that ΔC.S. values reflect the average chemical shift of both populations of molecules. At increasing SMT concentrations, ΔC.S. values reflect the increase in drug fraction inside the membrane. At the highest drug:lipid ratio, SMT peaks were considerably shifted (up to 0.12 ppm for peak **e**) and many of them were affected by the membrane environment, specially the methylene (**e** and **f**) and the indole ring (**g**, **i**, **h**, **j**) hydrogen nuclei.

The observed ΔC.S. are consistent with results of previous MD simulations in POPC bilayers (Wood and Pickholz, 2013), where SMT have displayed interfacial distribution and interaction with polar head groups of POPC. The correlation between drug:lipid ratio and ΔC.S. suggests that the interaction is greater with increasing number of molecules of SMT at the interface and the whole system. Moreover, SMT results are comparable with other amphiphilic compounds (local anesthetics, as lidocaine and mepivacaine mainly (Fraceto et al., 2005)) which affect the choline and phosphate hydrogen nuclei of EPC in the same direction.

The presence of SMT in-between the EPC molecules may also induce changes in the dynamics of the lipids, which can be accompanied by longitudinal relaxation time experiments (Fraceto et al., 2002; Fraceto et al., 2005). Using the inversion recovery technique, we have determined the longitudinal relaxation times (T_1) (Friebolin and Becconsall, 1993; Gerothanassis et al., 2002) for those SMT and EPC peaks not overlapped in one-dimensional spectra (see Fig. 2). Fig. 4 shows the T_1 values for pure samples (SMT and EPC) and SMT:EPC mixtures, at three drug:lipid ratios (1:3, 1:2, 1:1). The T_1 values of pure EPC showed good agreement with other reports in the literature (Cabeça et al., 2009; Fraceto et al., 2002; Fraceto et al., 2005). T_1 values were small for the hydrogen nuclei at the polar head group, reflecting the restriction caused by electrostatic interactions between amine and phosphate groups of adjacent lipids (Fraceto et al., 2002). At the glycerol groups, hydrogen nuclei have intermediate mobility and in the hydrocarbon lipid chains the mobility increase towards the terminal methyl groups.

Fig. 4 reveals that, in all cases, the T_1 values of SMT:EPC samples decreased respect to the pure samples. The restricted mobility of SMT hydrogen nuclei is a clear evidence of drug partition into the membrane or membrane-water interface. The measured T_1 values represent not only the SMT molecules in the membranes, but also a fraction of the drug that is soluble in water. In the presence of EPC bilayer, we were able to identify that changes in T_1 values were more pronounced in the SMT hydrogen atoms belonging to the indole ring (peaks **h**, **i** and **g**)

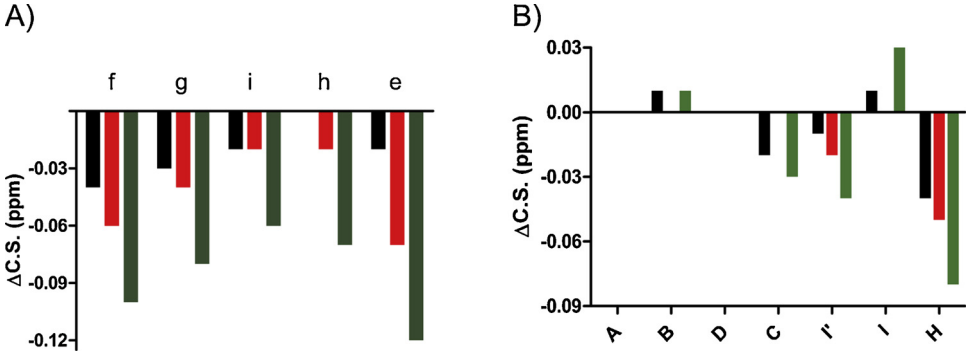

Fig. 3. ^{1}H NMR: changes in CS (ΔCS) of A) SMT (left) and B) EPC (right) hydrogen nuclei, at different SMT:EPC ratio: 1:3 black, 1:2 red and 1:1 green. (**Note:** although hydrogen nucleus **j** (SMT) shows a well-resolved peak (Fig. 2), it is not depicted here to follow the sequence of hydrogen nuclei in schematic skeleton structure (**j** is equivalent to peaks **g** or **i**, and shows similar ΔCS)). Assignments as in Fig. 2.

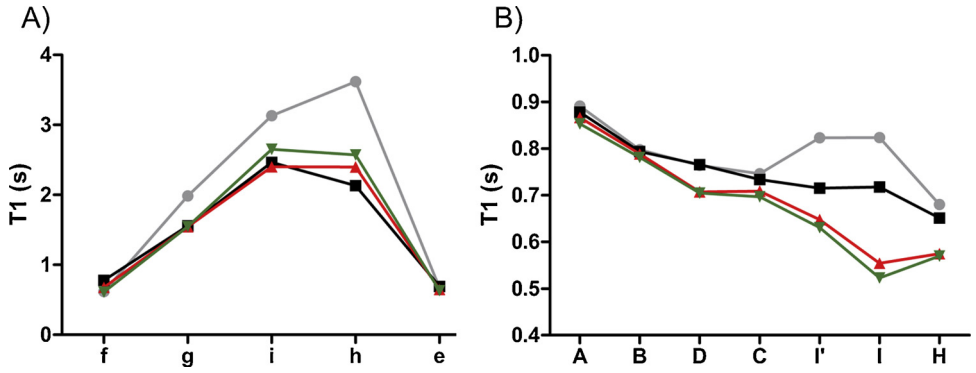

Fig. 4. Longitudinal relaxation times (T_1) of A) SMT (left) and B) EPC (right) hydrogen nuclei, at different SMT:EPC ratios: 1:3 - black, 1:2 - red and 1:1 -green. T_1 values for pure SMT and EPC samples are depicted in gray. Assignments as in Fig. 2.

(note: peak j was not shown, as explained above). As observed from ΔC.S. (Fig. 3), T_1 results confirmed that the indole group is the most affected region of SMT molecule upon partition into the membranes. The dynamics of peaks **e** and **f** did not show great T_1 variation when inside the membranes, probably because the mobility of those hydrogen nuclei was already restricted in the SMT molecule (T_1 values < 1 s) in aqueous phase, as a result of auto-interactions between SMT molecules. In that way, when hydrogen nuclei **e** and **f** got inserted at the polar head group region their mobility was just slightly affected. T_1 and CS account for different properties and they have different sensitivity. Nevertheless, both techniques are compatible with SMT partition into EPC liposomes.

In the presence of SMT, the T_1 values of hydrogen nuclei **I**, **I'** and **H** belonging to the EPC molecule decreased markedly (Fig. 4), indicating the effect of SMT on decreasing the mobility of the hydrogen nuclei from the polar head-groups (near to phosphocholine hydrogen nuclei), in a concentration dependent manner. These results suggest the insertion of SMT in the interfacial region of the bilayer, in line with the observed changes in chemical shifts (Fig. 3). In previous reports, we have already described a similar behavior for SMT as seen by MD simulations (Wood et al., 2018; Wood and Pickholz, 2013, 2014), showing preference for the interfacial region of POPC bilayers, revealing good agreement between NMR and MD results.

We have measured ROESY spectra of SMT:EPC mixtures, looking for intermolecular (through the space) magnetic transferences (building up NOE) (Bax and Davis, 1985; Friebolin and Becconsall, 1993; Gawrisch et al., 2002; Gerothanassis et al., 2002). Fig. 5 shows the ROESY spectrum for SMT:EPC (1:1) sample. We observed intermolecular correlations between several peaks, mostly corresponding to polar groups of SMT and EPC. Detection of short distances correlation (< 5 Å) NOE reveals intermolecular proximities between hydrogen atoms of SMT and EPC (choline) groups, as also observed before with other amphiphilic drugs (Bemporad et al., 2005). Among others, cross peaks between ^{1}H signals **c** and **G,** as well as between **d** and **H** can be observed from Fig. 5. Detection of NOE peaks did not rule out the existence of other interactions between SMT and EPC, such as those involving indole-ring hydrogen nuclei. By ROESY, the spatial correlation is detected between nuclei at a very short distance (2–5 Å), preventing detection of interactions involving bulky or rigid structures. This result is in agreement with the radial distribution of pSMT and POPC polar groups (peak at ≈2 Å) observed trough MD (Wood and Pickholz, 2013), in line with the requirement for ROESY inter-molecular correlation.

So far, we discussed NMR results depicting information about dynamics and distribution of SMT molecules in the SMT:EPC systems. The obtained results confirmed our previous findings regarding the interfacial distribution of SMT in membranes (from small angle x-ray scattering experiments) (Wood et al., 2018). Also NMR experiments allowed us to go further, studying in deeper detail specific interactions between SMT and EPC responsible for such distribution.

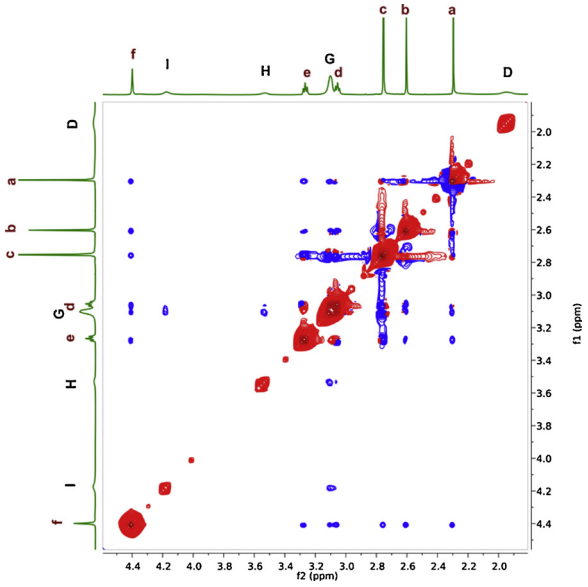

Fig. 5. ^{1}H-*ROESY* spectra of SMT:EPC 1:1 ratio. SMT peaks are referenced in red lowercase and EPC in black uppercase. Assignments as in Fig. 2.

Here, using NMR technique we were able to access to the behavior of protonated SMT specie in lipid liposomes. Considering that pKa of SMT is 9.7, it should be necessary to work at a pH around 12 in order to explore the effects of the neutral species. However, phosphatidylcholines are not stable at this pH (Austin et al., 2005, 1995; Boggara and Krishnamoorti, 2010; Boggara et al., 2012). Even more complex is to analyze the effect of both ionization states in mixtures (pH˜ 10) because of the NMR peaks overlapping. In this direction, MD simulations appear as a very powerful technique (Jemioła-Rzemińska et al., 2005), to explore the different conditions, leading to the prediction of experimental results (i.e. both species are present) and going further (i.e. neutral SMT).

3.2. pH dependence on the interaction of sumatriptan with model membranes

Here, we used classical MD simulations to address the pH dependence of SMT interaction with model membranes. Simulations were carried out for each ionization specie, and mixture of pSMT and nSMT in POPC bilayer under different conditions. Considering pKa of SMT and *Henderson-Hasselbach* equation, the studied systems consisted on: (1) ˜100% pSMT (simulating from low to physiological pH, (2) ˜100% nSMT (simulating pH over 11.7), (3) pSMT:nSMT 50:50 (simulating pH = pKa, ˜9.7) (Wellcome, 2001; Wojnar-Horton et al., 1996)

(Table 1). The drug molecules were initially placed in water. Besides, for the first case we also analyzed a different initial condition, in which pSMT was initially placed at the lipid core.

Simulations were run 150 ns. We have followed the convergence of the different properties. In this way, we used the last 50 ns for the average calculation for the results presented here, where the convergence was assured.

The *area per lipid, Alip,* was calculated as length of the simulation box in *x* dimension by length in *y* dimension, divided by number of lipids per monolayer, and is expressed in $Å^2$, with error in significant numbers. Fig. S2 (Supplementary information) shows *Alip* of the three systems, in which drugs were initially placed in the water phase, for the last 100 ns. When only one specie is present, the area per lipid was not affected (60.3(3) and 60.2(1)$Å^2$, for *pSMT* and *nSMT*, respectively). Nevertheless, the *Alip* increased when both ionization species were present going to 63.4(3)$Å^2$ (*npSMT*), suggesting cooperative behavior between them. A concomitant decreasing on membrane thickness (expressed as *z*-box dimension of POPC bilayer) was found for *npSMT*, showing little changes in the whole box volume (results not shown). Regarding lipid ordering, no differences were found for such property between *nSMT*, *pSMT* and *npSMT* systems.

Synergistic effects between nSMT and pSMT in the *npSMT* system, could be responsible for the increase on area per lipid. In order to see the drug organization within the bilayer, we evaluated the electron density profile (EDP) normal to the bilayer (z coordinate). Fig. 6 shows the EDPs (where z = 0 Å corresponds to the membrane center). From this figure one can observe that SMT molecules partition between the water phase and the lipid-water interface. The main difference between nSMT and pSMT partition was that nSMT entered deeper into the membrane, without reaching the membrane core (Jemioła-Rzemińska et al., 2005). Besides, no crossing (from one bilayer leaflet to the other one) events were observed for any of the drugs, during the entire simulation time. The coexistence of both SMT species in the same bilayer (*npSMT*) leads to a very similar behavior regarding distribution. The percentage of molecules at the aqueous phase differed between the conditions (see Table S2, Supplementary material), as observed in similar system containing naratriptan (NRT) (Wood and Pickholz, 2016). nSMT showed a bimodal distribution at the interface, locating near to glycerol groups of POPC and at the water phase, with relatively poor

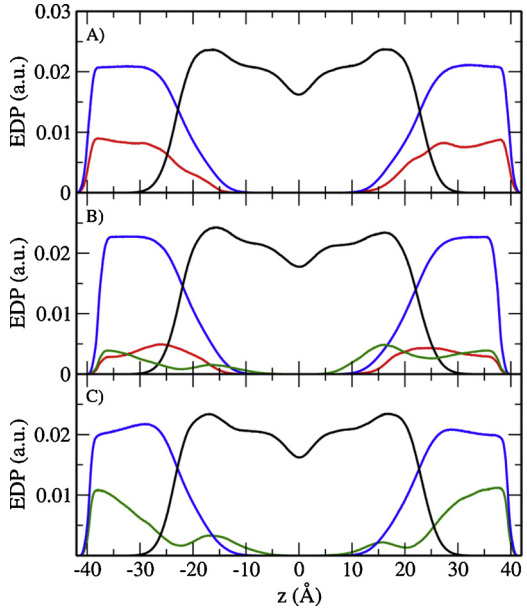

Fig. 6. Electron density profiles. Drug densities are depicted in: A) pSMT (red) (*pSMT*); B) *npSMT*: red for pSMT, green for nSMT, C) nSMT (green) (*nSMT*); (drug density scaled twice). For A), B) and C) POPC is depicted in black and water in blue.

partition nearby the phosphate groups, while pSMT had a continuous distribution through the entire interface and water regions. The particular behavior of the different ionization species could also affect the bilayer organization, lipid area and hydration of lipid head groups, as was previously discussed for NRT (Wood and Pickholz, 2016).

In order to analyze the specific orientation of the sumatriptan molecules within the bilayer, the EDP of different SMT groups was calculated. In Fig. 7 we show the results for dimethyl amino ethyl (ionizable group), pyrrole ring of indole (bearing the –NH group), benzene ring of indole and sulfonamide. For the neutral molecules, we observed that at interfaces nSMT shows specific orientation where the dimethyl amino ethyl and, in less extent, sulfonamide groups entered deeper into the bilayer core. On the other hand, pSMT did not show, in average, any specific orientation. Furthermore, in the *npSMT* system, both neutral and protonated molecules followed similar behavior to those observed for *nSMT* and *pSMT* systems. A snapshot of this system is shown as Fig. S3 in SI.

Regarding drug-lipid polar head interactions, in previous work we found three possible mechanisms: salt bridges, cation-π and hydrogen bonds (Wood and Pickholz, 2013, 2014, 2016). Next, we show the analysis of pair interactions between SMT and POPC molecules, illustrating some of the mentioned mechanisms.

First, the existence of non-covalent cation–π interactions (Petersen et al., 2005; Wood et al., 2013), was estimated for all the studied cases. An important implication of cation-π interaction is that indole molecules, such as serotonin and its precursors, adopt an interfacial location in lipid bilayers (Wood et al., 2013). The indole ring is a π-electron rich aromatic system with hydrogen bond donor character (given by the -NH group that is able to establish cation-π interactions) (Mecozzi et al., 1996). This kind of interaction was studied from the radial distribution function (g(r)), as previously reported (Petersen et al., 2005; Wood et al., 2013; Wood and Pickholz, 2013). The calculated $g_{cation\text{-}\pi}(r)$ functions are shown in Fig. 8A. We can see a well-defined peak at ≈4.0 Å for all the three cases, and apparently stronger for the *npSMT* case. In a similar way, g(r) for the indole group is shown in Fig. S4, suggesting that cooperative effects of both coexisting ionization species (pSMT and nSMT) in *npSMT* increase this kind of interaction.

In addition, we have simulated the *pSMTc* system, where pSMT molecules were initially placed inside the bilayer (last system in Table 1). Following the EDP of the bilayer components (Fig. S5), we found that SMT converged to an interfacial distribution in ˜60 ns. In this way, the distribution of pSMT molecules dis not change regarding the initial condition. This result suggests that polar (dimethyl amino ethyl and sulfonamide) and indole groups determine SMT orientation, by performing simultaneous interaction with the lipid head groups. Finally, differently than observed with protonated naratriptan species (Wood and Pickholz, 2016), pSMT molecules did not form aggregates in the hydrophobic core. In this regard, it is important to mention that, despite the high number of drug molecules in the simulated systems, no aggregates were found in the water phase.

4. Conclusions

In this work we investigated the distribution of sumatriptan in lipid bilayers, through different NMR techniques and by MD simulations.

^{1}H NMR experiments showed significant variations in the chemical shift of SMT hydrogen nuclei in the presence of EPC, and *vice versa*, in a concentration dependent manner. The major shifts were observed for the hydrogen nuclei at the polar groups of EPC, confirming the interaction of SMT with this interfacial region as was previously shown (Wood and Pickholz, 2013). Spin-lattice relaxation (T_1) measurements provided information about the dynamics of different depths of the bilayer, in the absence and presence of SMT, depicting lipid bilayer anisotropy. The differences observed between T_1 values also confirmed interaction of the anti-migraine drug with the phospholipid bilayer, with a preferential localization of SMT in the polar lipid head-groups. In

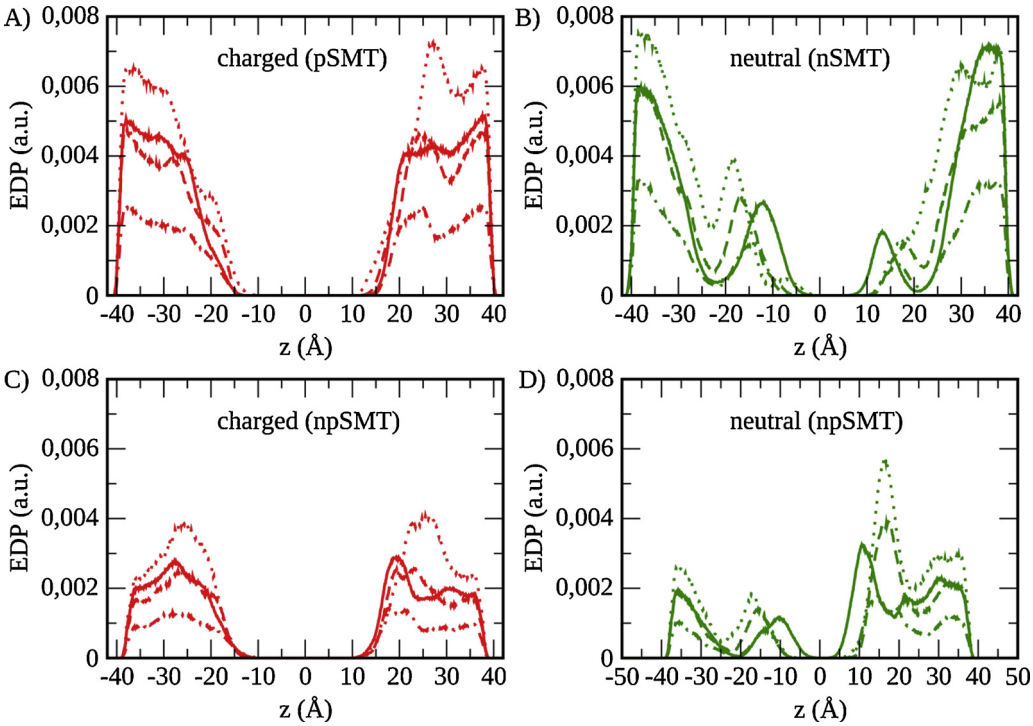

Fig. 7. EDP of SMT groups: dimethyl amino ethyl (solid line), sulfonamide (dotted lines), benzene ring of indole (dashed lines) and pyrrol ring of indole (dotted-dashed) in A) *pSMT* system, B) *nSMT* system, C) pSMT molecules of *npSMT* system and D) nSMT molecules of *npSMT* system.

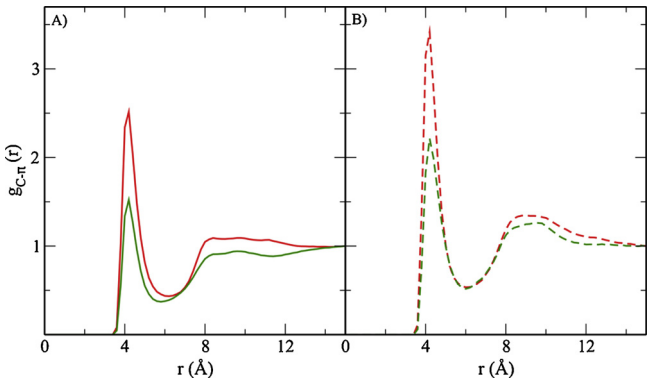

Fig. 8. g(r) cation-π of A) pSMT red (*pSMT)*, solid lines; nSMT green (*nSMT*), solid lines, B) *npSMT*: dashed red for pSMT and dashed green for nSMT.

addition, NMR results revealed that indole hydrogen nuclei is in a more restricted environment after insertion in-between lipids, with the aromatic ring (the bulky part of SMT) laying down in the vicinity of glycerol and choline groups, as observed for other amphiphilic drugs (Fraceto et al., 2002; Fraceto et al., 2005). This preferential insertion explains why SMT partition affects mainly the hydrogen nuclei of choline, phosphate and even glycerol moieties. Nuclear Overhauser effect experiments allowed determination of short-distance correlation peaks between polar groups of SMT and EPC choline hydrogen nuclei. This location could affect interactions between polar head groups of adjacent lipids and the mobility of lipids in the bilayer. A more comprehensive view was obtained from MD simulations results, which accurate atomistic representation revealed details on the drug molecular conformation within the bilayer.

In this sense, we used MD simulations to simultaneously validate some NMR results and to further explore situations unreachable from the experimental point of view, such as absolute nSMT (very high pH). We found that neutral SMT, as protonated SMT, essentially partitions between the water and lipid/water interface. When neutral and protonated species coexist in the simulation, a combination of results was observed along with a lateral expansion of the simulation box, due to the simultaneous presence of both species.

In summary, we fully addressed by the complementarity of NMR and MD techniques the localization of SMT in lipid bilayers, as previously predicted (Wood et al., 2018; Wood and Pickholz, 2013, 2014). We found good agreement for the observed changes in model bilayers, due to the presence of SMT at different concentrations. We also study in deep details the dynamic properties to fully characterize SMT:PC systems through NMR and MD simulations. This approach confirmed the SMT preference for the interface region of the bilayer, in which the drug adopts a preferential conformation through interactions between polar and electron-rich groups, as suggested for other drugs (Bemporad et al., 2005). Altogether, these results highlight the importance of studying distribution of drugs in dynamical and non-homogeneous systems and reveal the limitations of SMT to cross lipid membranes. Since the amphiphilic and ionizable characters of SMT, plus an intriguing pharmacokinetic and pharmacodynamics, could be useful to understand biophysical and pharmacokinetic behavior of similar drugs across interfaces, during drug design and preclinical studies.

Declaration of Competing Interest

The authors of this manuscript do not have any conflicts of interest to declare

Acknowledgements

The authors would like to acknowledge IQUIMEFA (CONICET-UBA) for NMR facility; LF for performing, processing and interpretation of NMR experiments; LAFEDAR for the donation of Sumatriptan Succinate; CONICET and Conselho Nacional Pesquisa (CNPq/Brazil, #1420869/2016-6) for the financial support.

Appendix A. Supplementary data

Supplementary material related to this article can be found, in the online version, at doi:https://doi.org/10.1016/j.chemphyslip.2019.104792.

References

Ahn, A.H., Basbaum, A.I., 2005. Where do triptans act in the treatment of migraine? Pain 115, 1.

Andersen, H.C., 1980. Molecular dynamics simulations at constant pressure and/or temperature. J. Chem. Phys. 72, 2384–2393.

Austin, R.P., Barton, P., Davis, A.M., Fessey, R.E., Wenlock, M.C., 2005. The thermodynamics of the partitioning of ionizing molecules between aqueous buffers and phospholipid membranes. Pharm. Res. 22, 1649–1657.

Austin, R.P., Davis, A.M., Manners, C.N., 1995. Partitioning of ionizing molecules between aqueous buffers and phospholipid vesicles. J. Pharm. Sci. 84, 1180–1183.

Avdeef, A., Box, K., Comer, J., Hibbert, C., Tam, K., 1998. pH-metric logP 10. Determination of liposomal membrane-water partition coefficients of lonizable drugs. Pharm. Res. 15, 209–215.

Bax, A., Davis, D.G., 1985. Practical aspects of two-dimensional transverse NOE spectroscopy. J. Magn. Reson. 63, 207–213.

Bemporad, D., Luttmann, C., Essex, J., 2005. Behaviour of small solutes and large drugs in a lipid bilayer from computer simulations. Biochim. Biophys. Acta (BBA)-Biomembr. 1718, 1–21.

Boggara, M.B., Krishnamoorti, R., 2010. Partitioning of nonsteroidal antiinflammatory drugs in lipid membranes: a molecular dynamics simulation study. Biophys. J. 98, 586–595.

Boggara, M.B., Mihailescu, M., Krishnamoorti, R., 2012. Structural association of nonsteroidal anti-inflammatory drugs with lipid membranes. J. Am. Chem. Soc. 134, 19669–19676.

Cabeça, L.F., Pickholz, M., de Paula, E., Marsaioli, A.J., 2009. Liposome-prilocaine interaction mapping evaluated through STD NMR and molecular dynamics simulations. J. Phys. Chem. B 113, 2365–2370.

Campbell, S.D., Regina, K.J., Kharasch, E.D., 2014. Significance of lipid composition in a blood-brain barrier-mimetic PAMPA assay. J. Biomol. Screen. 19, 437–444.

Carpenter, T.S., Kirshner, D.A., Lau, E.Y., Wong, S.E., Nilmeier, J.P., Lightstone, F.C., 2014. A method to predict blood-brain barrier permeability of drug-like compounds using molecular dynamics simulations. Biophys. J. 107, 630–641.

Coimbra, J.T., Brás, N.F., Fernandes, P.A., Rangel, M., Ramos, M.J., 2018. Membrane partition of bis-(3-hydroxy-4-pyridinonato) zinc (ii) complexes revealed by molecular dynamics simulations. RSC Adv. 8, 27081–27090.

Coimbra, J.T., Moniz, T., Brás, N.F., Ivanova, G., Fernandes, P.A., Ramos, M.J., Rangel, M., 2014. Relevant interactions of antimicrobial iron chelators and membrane models revealed by nuclear magnetic resonance and molecular dynamics simulations. J. Phys. Chem. B 118, 14590–14601.

Chew, C.F., Guy, A., Biggin, P.C., 2008. Distribution and dynamics of adamantanes in a lipid bilayer. Biophys. J. 95, 5627–5636.

Dave, R.A., Morris, M.E., 2016. Novel high/low solubility classification methods for new molecular entities. Int. J. Pharm. 511, 111–126.

de Paula, E., Schreier, S., 1996. Molecular and physicochemical aspects of local anesthetic-membrane interaction. Braz. J. Med. Biol. Res. 29, 877–894.

Edvinsson, L., Tfelt-Hansen, P., 2008. The blood-brain barrier in migraine treatment. Cephalalgia 28, 1245–1258.

Essmann, U., Perera, L., Berkowitz, M.L., Darden, T., Lee, H., Pedersen, L.G., 1995. A smooth particle mesh Ewald method. J. Chem. Phys. 103, 8577–8593.

Feller, S.E., MacKerell, A.D., 2000. An improved empirical potential energy function for molecular simulations of phospholipids. J. Phys. Chem. B 104, 7510–7515.

Feller, S.E., Zhang, Y., Pastor, R.W., Brooks, B.R., 1995. Constant pressure molecular dynamics simulation: the Langevin piston method. J. Chem. Phys. 103, 4613–4621.

Fraceto, L.F., de Matos Alves Pinto, L., Franzoni, L., Albert Carmo Braga, A., Spisni, A., Schreier, S., de Paula, E., 2002. Spectroscopic evidence for a preferential location of lidocaine inside phospholipid bilayers. Biophys. Chem. 99, 229–243.

Filip, M., Bader, M., 2009. Overview on 5-HT receptors and their role in physiology and pathology of the central nervous system. Pharmacol. Rep. 61, 761–777.

Fraceto, L.F., Spisni, A., Schreier, S., de Paula, E., 2005. Differential effects of uncharged aminoamide local anesthetics on phospholipid bilayers, as monitored by 1 H-NMR measurements. Biophys. Chem. 115, 11–18.

Friebolin, H., Becconsall, J.K., 1993. Basic One-and Two-Dimensional NMR Spectroscopy. VCH, Weinheim.

Fulmer, G.R., Miller, A.J.M., Sherden, N.H., Gottlieb, H.E., Nudelman, A., Stoltz, B.M., Bercaw, J.E., Goldberg, K.I., 2010. NMR chemical shifts of trace impurities: common laboratory solvents, organics, and gases in deuterated solvents relevant to the organometallic chemist. Organometallics 29, 2176–2179.

Gawrisch, K., Eldho, N.V., Polozov, I.V., 2002. Novel NMR tools to study structure and dynamics of biomembranes. Chem. Phys. Lipids 116, 135–151.

Gerothanassis, I.P., Troganis, A., Exarchou, V., Barbarossou, K., 2002. Nuclear magnetic resonance (NMR) spectroscopy: basic principles and phenomena, and their applications to chemistry, biology and medicine. Chem. Educ. Res. Pract. 3, 229–252.

Gil, V.M., Geraldes, C.Fd.G.C., 1987. Ressonância magnética nuclear: fundamentos, métodos e aplicações.

Gregoriadis, G., 1992. Liposome Technology, second edition. Taylor & Francis.

Hoff, B., Strandberg, E., Ulrich, A.S., Tieleman, D.P., Posten, C., 2005. 2H-NMR study and molecular dynamics simulation of the location, alignment, and mobility of pyrene in POPC bilayers. Biophys. J. 88, 1818–1827.

Jemioła-Rzemińska, M., Pasenkiewicz-Gierula, M., Strzałka, K., 2005. The behaviour of beta-carotene in the phosphatidylcholine bilayer as revealed by a molecular simulation study. Chem. Phys. Lipids 135, 27–37.

Johnston, M.M., Rapoport, A.M., 2010. Triptans for the management of migraine. Drugs 70, 1505–1518.

Jorgensen, W.L., Chandrasekhar, J., Madura, J.D., Impey, R.W., Klein, M.L., 1983. Comparison of simple potential functions for simulating liquid water. J. Chem. Phys. 79, 926–935.

Kalé, L., Skeel, R., Bhandarkar, M., Brunner, R., Gursoy, A., Krawetz, N., Phillips, J., Shinozaki, A., Varadarajan, K., Schulten, K., 1999. NAMD2: greater scalability for parallel molecular dynamics. J. Comput. Phys. 151, 283–312.

Kopeć, W., Telenius, J., Khandelia, H., 2013. Molecular dynamics simulations of the interactions of medicinal plant extracts and drugs with lipid bilayer membranes. FEBS J. 280, 2785–2805.

Kuroda, Y., Fujiwara, Y., 1987. Locations and dynamical perturbations for lipids of cationic forms of procaine, tetracaine, and dibucaine in small unilamellar phosphatidylcholine vesicles as studied by nuclear Overhauser effects in 1H nuclear magnetic resonance spectroscopy. Biochim. Biophys. Acta (BBA)-Biomembr. 903, 395–410.

Kuroda, Y., Kitamura, K., 1984. Intra-and intermolecular proton-proton nuclear Overhauser effect studies on the interactions of chlorpromazine with lecithin vesicles. J. Am. Chem. Soc. 106, 1–6.

Lopes, D., Jakobtorweihen, S., Nunes, C., Sarmento, B., Reis, S., 2017. Shedding light on the puzzle of drug-membrane interactions: experimental techniques and molecular dynamics simulations. Prog. Lipid Res. 65, 24–44.

MacKerell Jr, A.D., Bashford, D., Bellott, M., Dunbrack Jr, R.L., Evanseck, J.D., Field, M.J., Fischer, S., Gao, J., Guo, H., Ha, S., Joseph-McCarthy, D., Kuchnir, L., Kuczera, K., Lau, F.T.K., Mattos, C., Michnick, S., Ngo, T., Nguyen, D.T., Prodhom, B., Reiher Iii, W.E., Roux, B., Schlenkrich, M., Smith, J.C., Stote, R., Straub, J., Watanabe, M., Wiórkiewicz-Kuczera, J., Yin, D., Karplus, M., 1998. All-atom empirical potential for molecular modeling and dynamics studies of proteins. J. Phys. Chem. B 102, 3586–3616.

Martinez, L., Andrade, R., Birgin, E.G., Martínez, J.M., 2009. PACKMOL: a package for building initial configurations for molecular dynamics simulations. J. Comput. Chem. 30, 2157–2164.

Mecozzi, S., West, A.P., Dougherty, D.A., 1996. Cation-pi interactions in aromatics of biological and medicinal interest: electrostatic potential surfaces as a useful qualitative guide. Proc. Natl. Acad. Sci. U. S. A. 93, 10566–10571.

Negro, A., Koverech, A., Martelletti, P., 2018. Serotonin receptor agonists in the acute treatment of migraine: a review on their therapeutic potential. J. Pain Res. 11, 515.

Paquet, M., Fournier, I., Barwicz, J., Tancrède, P., Auger, M., 2002. The effects of amphotericin B on pure and ergosterol-or cholesterol-containing dipalmitoylphosphatidylcholine bilayers as viewed by 2 H NMR. Chem. Phys. Lipids 119, 1–11.

Peetla, C., Bhave, R., Vijayaraghavalu, S., Stine, A., Kooijman, E., Labhasetwar, V., 2010. Drug resistance in breast cancer cells: biophysical characterization of and doxorubicin interactions with membrane lipids. Mol. Pharm. 7, 2334–2348.

Petersen, F.N., Jensen, M., Nielsen, C.H., 2005. Interfacial tryptophan residues: a role for the cation-pi effect? Biophys. J. 89, 3985–3996.

Santos, N.C., Prieto, M., Castanho, M.A., 2003. Quantifying molecular partition into model systems of biomembranes: an emphasis on optical spectroscopic methods. Biochim. Biophys. Acta (BBA)-Biomembr. 1612, 123–135.

Schreier, S., Frezzatti Jr, W.A., Araujo, P.S., Chaimovich, H., Cuccovia, I.M., 1984. Effect of lipid membranes on the apparent pK of the local anesthetic tetracaine. Spin label and titration studies. Biochim. Biophys. Acta 769, 231–237.

Selivonchick, D.P., Roots, B.I., 1977. Lipid and fatty acyl composition of rat brain capillary endothelia isolated by a new technique. Lipids 12, 165–169.

Shidhaye, S.S., Saindane, N.S., Sutar, S., Kadam, V., 2008. Mucoadhesive bilayered patches for administration of sumatriptan succinate. AAPS PharmSciTech 9, 909–916.

Smith, R.L., Oldfield, E., 1984. Dynamic structure of membranes by deuterium NMR. Science 225, 280–288.

Tanaka, A., Furubayashi, T., Tomisaki, M., Kawakami, M., Kimura, S., Inoue, D., Kusamori, K., Katsumi, H., Sakane, T., Yamamoto, A., 2017. Nasal drug absorption from powder formulations: the effect of three types of hydroxypropyl cellulose (HPC). Eur. J. Pharm. Sci. 96, 284–289.

Tfelt-Hansen, P., De Vries, P., Saxena, P.R., 2000. Triptans in migraine. Drugs 60, 1259–1287.

Tfelt-Hansen, P.C., 2010. Does sumatriptan cross the blood-brain barrier in animals and man? J. Headache Pain 11, 5–12.

Tuckerman, M.E., Berne, B.J., Martyna, G.J., 1991. Molecular dynamics algorithm for multiple time scales: systems with long range forces. J. Chem. Phys. 94, 6811–6815.

Udutha, S., Shankar, G., Borkar, R.M., Kumar, K., Srinivasulu, G., Guntuku, L., Naidu, V., Srinivas, R., 2018. Identification and characterization of stress degradation products of sumatriptan succinate by using LC/Q-TOF-ESI-MS/MS and NMR: toxicity evaluation of degradation products. J. Mass Spectrom. 53, 963–975.

Venable, R.M., Krämer, A., Pastor, R.W., 2019. Molecular dynamics simulations of membrane permeability. Chem. Rev. 119, 5954–5997.

Wellcome, G., 2001. Imitrex®(Sumatriptan Succinate) Injection Prescribing Information. Research Triangle Park, NC. .

Wohlert, J., Edholm, O., 2006. Dynamics in atomistic simulations of phospholipid membranes: nuclear magnetic resonance relaxation rates and lateral diffusion. J. Chem. Phys. 125, 204703.

Wojnar-Horton, R.E., Hackett, L.P., Yapp, P., Dusci, L.J., Paech, M., Ilett, K.F., 1996. Distribution and excretion of sumatriptan in human milk. Br. J. Clin. Pharmacol. 41, 217–221.

Wood, I., Albano, J.M., Pedro Filho, L., Couto, V.M., de Farias, M.A., Portugal, R.V., de

Paula, E., Oliveira, C.L., Pickholz, M., 2018. A sumatriptan coarse-grained model to explore different environments: interplay with experimental techniques. Eur. Biophys. J. 1–11.
Wood, I., Martini, M.F., Pickholz, M., 2013. Similarities and differences of serotonin and its precursors in their interactions with model membranes studied by molecular dynamics simulation. J. Mol. Struct. 1045, 124–130.
Wood, I., Pickholz, M., 2013. Concentration effects of sumatriptan on the properties of model membranes by molecular dynamics simulations. Eur. Biophys. J. 42, 833–841.
Wood, I., Pickholz, M., 2014. Triptan partition in model membranes. J. Mol. Model. 20, 2463.
Wood, I., Pickholz, M., 2016. Naratriptan aggregation in lipid bilayers: perspectives from molecular dynamics simulations. J. Mol. Model. 22, 221.
Wormald, M.R., Petrescu, A.J., Pao, Y.-L., Glithero, A., Elliott, T., Dwek, R.A., 2002. Conformational studies of oligosaccharides and glycopeptides: complementarity of NMR, X-ray crystallography, and molecular modelling. Chem. Rev. 102, 371–386.
Zhang, J., Hadlock, T., Gent, A., Strichartz, G.R., 2007. etracaine-membrane interactions: effects of lipid composition and phase on drug partitioning, location, and ionization. Biophys J. 92, 3988–4001.